Gels

Deutsche Ausgabe: DOI: 10.1002/ange.201608413
Internationale Ausgabe: DOI: 10.1002/anie.201608413

Metal–Phenolic Supramolecular Gelation

*Md. Arifur Rahim, Mattias Björnmalm, Tomoya Suma, Matthew Faria, Yi Ju, Kristian Kempe, Markus Müllner, Hirotaka Ejima, Anthony D. Stickland, and Frank Caruso**

Abstract: *Materials assembled by coordination interactions between naturally abundant polyphenols and metals are of interest for a wide range of applications, including crystallization, catalysis, and drug delivery. Such an interest has led to the development of thin films with tunable, dynamic properties, however, creating bulk materials remains a challenge. Reported here is a class of metallogels formed by direct gelation between inexpensive, naturally abundant tannic acid and group(IV) metal ions. The metallogels exhibit diverse properties, including self-healing and transparency, and can be doped with various materials by in situ co-gelation. The robustness and flexibility, combined with the ease, low cost, and scalability of the coordination-driven assembly process make these metallogels potential candidates for chemical, biomedical, and environmental applications.*

Functional materials in nature are assembled under ambient conditions from a limited selection of components; however, they display remarkably complex and dynamic behavior.[1–3] A prominent example is mussel byssal threads, which form hard but flexible coatings through metal–phenolic coordination.[4] We recently demonstrated that metal–phenolic complexation between different metals and phenolic ligands can be used to assemble conformal coatings, thus yielding thin films and particles with tailored properties.[5–7] Metal–phenolic complexation is also of interest for the assembly of bulk materials, such as supramolecular biomaterials and gels:[8–10] 3,4-dihydroxyphenylalanine-modified peptides and polyethylene glycol were complexed with di- or trivalent transition metals (e.g., Fe^{III}) to assemble metal–phenolic gels.[11–15] However, the assembly of such gels requires the use of synthetic, pre-synthesized macromolecular building blocks.[11–15] While polyphenol-based gels can be assembled using non-coordination interactions, for example between tannic acid (TA) and polymers,[16,17] direct gelation between naturally occurring, unmodified polyphenols and metal ions is yet to be demonstrated.

Herein, we report the simple and rapid assembly of metal–phenolic gels (or metallogels) by the direct gelation of naturally occurring and inexpensive TA and group(IV) metal ions. The chemistry underlying this gelation is specific to group(IV) transition metals. We use the gelation between TA and Ti^{IV} as a primary example to demonstrate the formation of metallogels and their properties. These metallogels can form in different organic solvents and aqueous solutions through simple mixing at a range of molar ratios. Furthermore, these gels can be engineered to exhibit tunable mechanical properties, optical transparency, injectability, moldability, shape persistence, adhesiveness, and self-healing properties, and to have stability in the pH range of 2–10. Both TA and Ti are known to be highly biocompatible, with TA being a natural antioxidant and Ti being extensively used in clinical implants.[18] This gelation process is robust and the metallogels can be doped in situ by co-gelation with various materials to endow them with application-specific properties.

The polyphenolic structure of TA consists of five digalloyl ester groups covalently attached to a central glucose core (Figure 1a). The galloyl functional groups of TA provide multitopic chelating sites which can coordinate a range of transition metals.[6] Solutions of TA and Ti^{IV} formed gels after mixing, and such gelation occurred in diverse organic and aqueous solvents including *N*-methyl-2-pyrrolidone (NMP), *N*,*N*-dimethylformamide (DMF), and water (Figure 1b–h). The organogels are denoted as "TA-Ti^{IV}-OG (solvent)" and the hydrogels as "TA-Ti^{IV}-HG".

The orange-red TA-Ti^{IV} sol (Figure 1d) formed an optically transparent dark-red gel upon standing at room temperature (21–24 °C), as demonstrated by the tube/vial inversion test (Figure 1e–h). The gelation time could be tuned from minutes to weeks by changing the concentration of TA and the molar ratio of TA to Ti^{IV} (see Figures S1 and S2 in the Supporting Information). The gelation behavior could also be controlled by using sonication and heating; both processes reduced the gelation time (see Figure S1). Notably, no gelation was observed for the TA-Ti^{IV}-OG (NMP) system prepared at a TA/Ti^{IV} molar ratio of 1:1, even when the TA concentration was increased to 20 wt.% (see Figure S1). Furthermore, the combination of TA with other first-row

[*] M. A. Rahim, M. Björnmalm, T. Suma, M. Faria, Y. Ju, Dr. K. Kempe, Dr. M. Müllner, Dr. H. Ejima, Prof. F. Caruso
ARC Centre of Excellence in Convergent Bio-Nano Science and Technology, and the Department of Chemical and Biomolecular Engineering, The University of Melbourne
Parkville, Victoria 3010 (Australia)
E-mail: fcaruso@unimelb.edu.au
Dr. A. D. Stickland
Particulate Fluids Processing Centre, Department of Chemical and Biomolecular Engineering, The University of Melbourne
Parkville, Victoria 3010 (Australia)
Dr. K. Kempe
Present address: ARC Centre of Excellence in Convergent Bio-Nano Science and Technology
Monash Institute of Pharmaceutical Sciences, Monash University
Parkville, Victoria 3052 (Australia)
Dr. M. Müllner
Present address: School of Chemistry, The University of Sydney
Sydney, New South Wales 2006 (Australia)
Dr. H. Ejima
Present address: Institute of Industrial Science
The University of Tokyo, 4-6-1 Komaba, Meguro-ku, Tokyo (Japan)
Supporting information and the ORCID identification number(s) for the author(s) of this article can be found under: http://dx.doi.org/10.1002/anie.201608413.

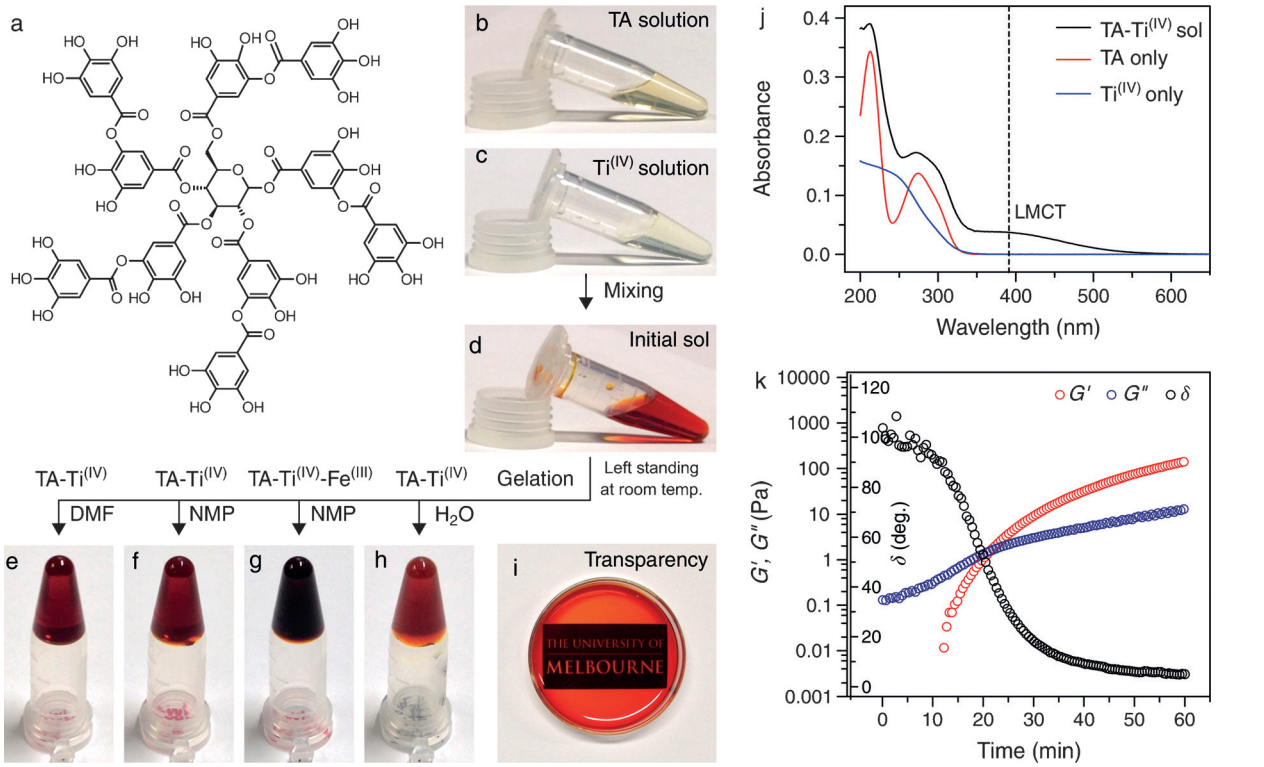

Figure 1. Gelation of the TA-Ti^{IV} gel system. a) Structure of TA containing multiple chelating sites (galloyl groups). Mixing of the TA solution (b) with Ti^{IV} solution (c) produces an orange-red TA-Ti^{IV} sol (d). e–h) Subsequent gelation in different solvents. i) TA-Ti^{IV}-OG (NMP) thin gel prepared on a glass Petri dish. j) UV/Visible absorption spectrum of a TA-Ti^{IV} sol. Absorption spectra of TA and Ti^{IV} solutions are also shown. k) Dynamic oscillatory rheological measurement showing the sol-gel transition of the TA-Ti^{IV} gel system.

transition metals (under similar conditions) did not result in gelation (see Figures S3 and S4), suggesting that the direct gelation is specific to group(IV) metal ions. In particular, the gelation of TA and Fe^{III} was unsuccessful (see Figure S3), and is consistent with a previous study.[16] However, Fe^{III} and other metals could be incorporated in situ in the TA-Ti^{IV} matrix by co-gelation (Figure 1 g). This approach allowed fabrication of a wide range of functional materials, some of which are explored below. The gelation behavior of TA-Ti^{IV}-HG prepared at different TA concentrations and stoichiometries is presented in Figure S2. The gelation times of the TA-Ti^{IV}-HG system were faster than those of the TA-Ti^{IV}-OG system (see Figures S1 and S2). For example, using a TA/Ti^{IV} molar ratio of 1:4 and 5 wt.% TA, the gelation times were about 1 min and 1 h for TA-Ti^{IV}-HG and TA-Ti^{IV}-OG (NMP), respectively.

UV/Visible absorption spectroscopy performed on the TA/Ti^{IV} sols showed the characteristic ligand-to-metal charge-transfer (LMCT) band of TA-Ti^{IV} coordination (bis/tris-type in terms of the galloyl chelating sites) at $\lambda \approx 385$ nm (Figure 1 j).[19] Conversely, TA and Ti^{IV} solutions were featureless in the same spectral region (350–550 nm). The sol-to-gel transition of the TA-Ti^{IV}-OG (NMP) system was probed in situ by dynamic oscillatory rheology experiments (Figure 1 k). Initially, liquid-like (viscous) properties were observed, as evident from the higher loss modulus (G″) relative to the storage modulus (G′) (Figure 1 k). As time increased, the phase shift (δ) continued to decrease and G′ increased, indicating the solid-like (elastic) properties of the system. The sol-gel transition occurred when $G' > G''$ after the G′/G″ crossover point at about 20 min. When accounting for the time required for the experimental setup, this corresponds well with the observed gelation time (ca. 40 min) determined from the tube/vial inversion test.

To further investigate the TA-Ti^{IV}-OG (NMP) gel structure, X-ray photoelectron spectroscopy (XPS) was performed on the dried gels (Figure 2 a). C 1s, O 1s, and Ti 2p peaks were detected in the survey spectra (Figure 2 a). From the Ti 2p core-level photoelectron spectrum (Figure 2 b), Ti $2p_{3/2}$ and Ti $2p_{1/2}$ peaks were observed at binding energies of 459.3 and 465 eV, respectively, and were assigned to Ti^{IV} species in the gel.[20] Additionally, these results indicate the absence of redox reactions between TA and Ti^{IV} during gelation. As expected from the asymmetric multitopic structure of TA, the dried gels were amorphous, as determined by X-ray diffraction (XRD) (Figure 2 c).

The TA-Ti^{IV} gel system exhibits a combination of notable properties including shape persistence, high adhesive strength, load-bearing capability, and self-healing ability. These properties could be tuned by adjusting the composition and processing parameters of the gels. For example, the mechanical properties of the gels were changed by modifying the stoichiometry and concentration for a given solvent (Figure 2 d; see Figure S5). At a TA/Ti^{IV} molar ratio of 1:3, G′ of TA-Ti^{IV}-OG (NMP) increased from about 300 to 5000 Pa with increasing concentrations, as determined from the time

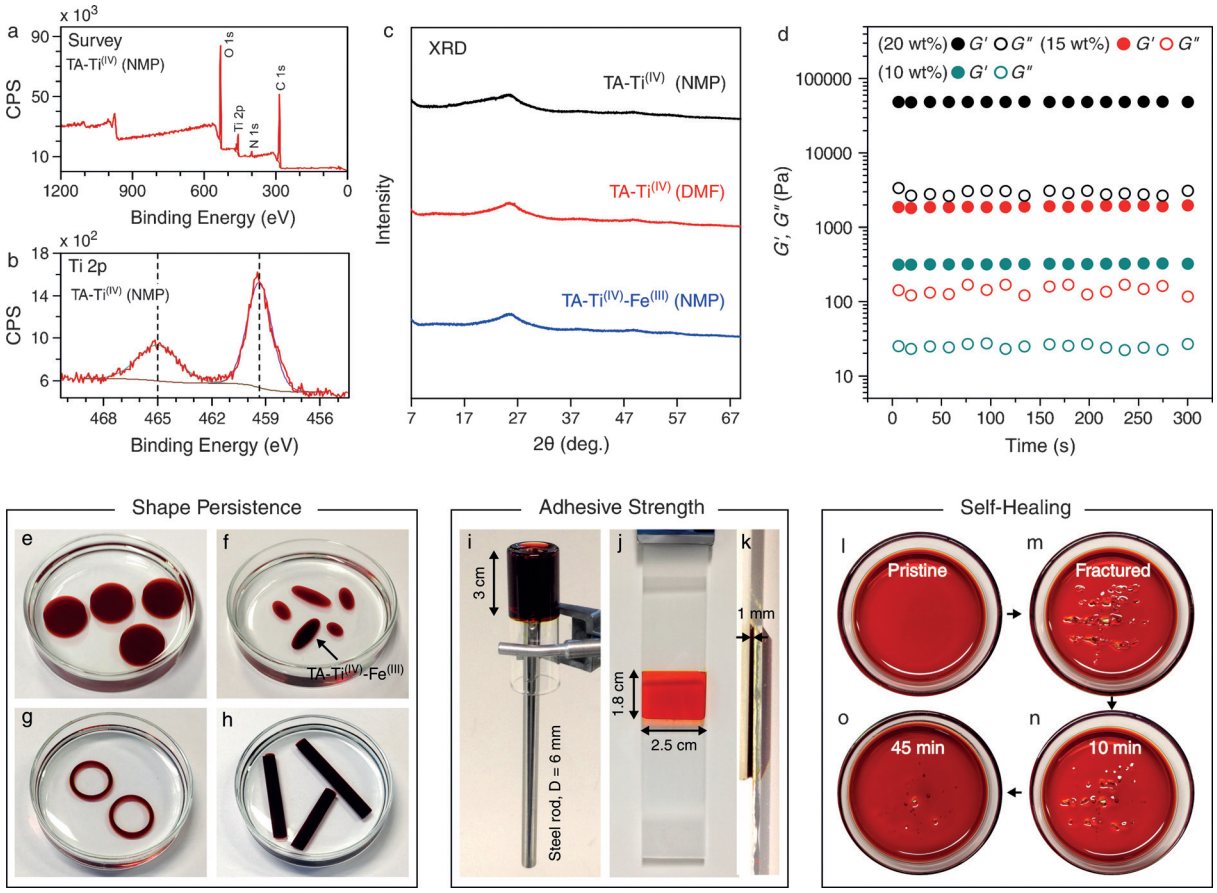

Figure 2. Characterization and properties of the TA-Ti^{IV} gels. a,b) XPS spectra of the dried TA-Ti^{IV}-OG (NMP) gels. c) XRD patterns of the dried TA-Ti^{IV} and TA-Ti^{IV}-Fe^{III} gels. d) Dynamic oscillatory rheological measurements of TA-Ti^{IV}-OG (NMP) prepared at different TA concentrations (TA/Ti^{IV} = 1:3). e–h) Shape of the gels: disc-shaped (e), oval (f), toroidal (g), and tubular (h). i) The load-bearing capability of the gels is demonstrated by holding an inverted steel rod in place. j,k) The high adhesive strength of the gels is demonstrated by preventing two glass plates from slipping. l–o) Self-healing properties of the gel [TA-Ti^{IV} (NMP), TA/Ti^{IV} = 1:2] monitored over time.

sweep tests (conducted at a frequency of 1 Hz and 1 % strain). At each concentration studied, G′ was greater than G″, suggesting the true gel nature of the materials prepared. The gels are moldable and demonstrate shape-persistence behavior (Figure 2e–h). Shape-persistent gels with a variety of shapes, including cylindrical, spherical, toroidal, triangular, and tubular, were obtained through molding, and no apparent changes in either the shape or size were observed over time (up to 3 months). The gels demonstrated high load-bearing capabilities and could hold loads of about 70 times greater than their own weight (i.e., a 0.45 g metallogel could hold a 30 g load; Figure 2i). Additionally, the adhesive capability of the gel was demonstrated by forming a thin (1 mm) gel layer between two glass plates; the gel prevented the glass plates from slipping (Figure 2j,k). In contrast to covalently bonded chemical gels, the dynamic nature of coordination bonding can endow self-healing properties in the resulting material.[11,16] Thus, the self-healing properties of the TA-Ti^{IV} gel system were investigated using a fracture-recovery test (Figure 2l–o). Gels formed in a glass Petri dish were fractured by a sharp blade and then allowed to stand unperturbed. The fractures healed over time and all visible traces of the fractures disappeared completely within 2 h.

The TA-Ti^{IV} gels are non-cytotoxic (see Figure S6) and are compatible with a range of environments and post-assembly processing treatments (Figure 3). For example, the gels could be made injectable (Figure 3a). Manual force on the piston of a syringe induced extrusion of the gel without clogging. Because of the high strain, the extruded gel was initially deformed but quickly self-repaired (Figure 3a,b). Furthermore, the gels could be dried to create monolithic xerogels and aerogels (Figure 3c,d). Moderate gel shrinkage was observed for the aerogels, whereas a substantial decrease in volume was observed for the xerogels. However, in both cases, volume shrinkage was homogenous without damage to the overall structure. The stability of the TA-Ti^{IV}-HG at various pH values was also investigated (Figure 3m). The hydrogel system was stable in the pH range of 2–10, suggesting strong coordination bonding between TA and Ti^{IV} in the gel. However, the hydrogel disassembled when subjected to pH values greater than 10 (see Figure S7).

A notable feature of TA-Ti^{IV} gel systems is their ability to incorporate diverse functional materials in the gel matrix by in situ co-gelation. The materials to be embedded can be mixed with the gel components in the initial TA-Ti^{IV} sol, and co-gelation generates composite gel materials: we investigated Fe^{III}, V^{III}, iron oxide magnetic nanoparticles (Fe_3O_4

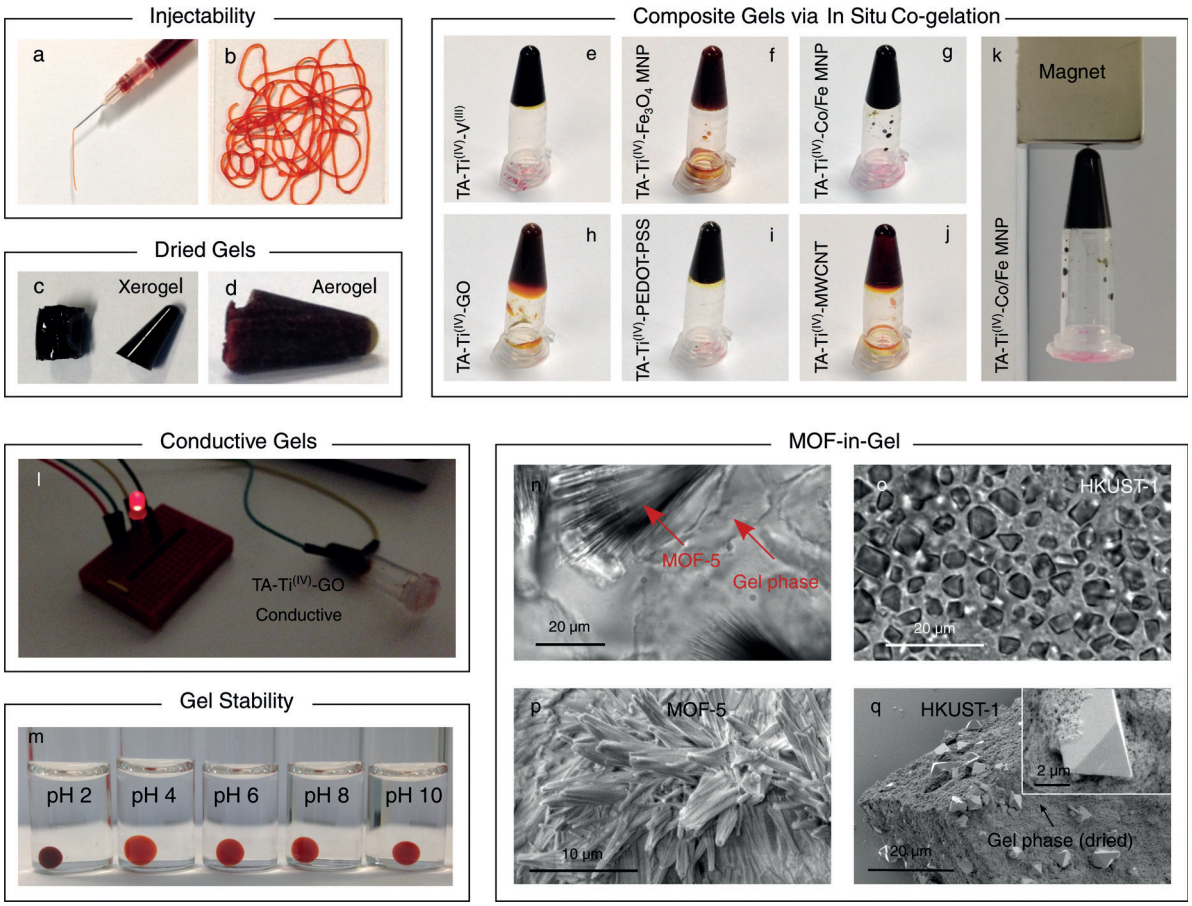

Figure 3. Properties of the TA-Ti^{IV} gel system. a,b) Injectable gel. c,d) Monolithic xerogels and aerogels prepared by solvent evaporation (c) and supercritical drying of the wet gels (d). e–j) Composite gels prepared by incorporating diverse materials via in situ co-gelation without affecting the fundamental gelation process. k) Magnetic behavior of the TA-Ti^{IV}-Co/Fe MNP system. l) Conductivity property of the TA-Ti^{IV}-GO system, which is capable of powering a light-emitting diode. m) Stability tests performed on the TA-Ti^{IV}-HG system that was exposed to different pH values. n,o) Differential interference contrast (DIC) images of MOF-5 and HKUST-1 crystallization in the TA-Ti^{IV} gel system. p,q) Scanning electron microscopy (SEM) characterization of MOF-5 and HKUST-1 crystallization in the TA-Ti^{IV} gel system.

MNP), cobalt ferrite magnetic nanoparticles (Co/Fe MNP), graphene oxide (GO), poly(3,4-ethylenedioxythiophene)-poly(styrenesulfonate) (PEDOT:PSS), and multiwalled carbon nanotubes (MWCNT; Figure 1g and Figure 3e–j). Gels loaded with Co/Fe MNP exhibited magnetism and those loaded with GO were conductive (Figure 3k,l). In contrast, the pristine gels did not exhibit any magnetic response or conductivity.

The robust nature of the prepared gel systems and the ability to add diverse dopants led us to consider more complex additives. The close relationship between the coordination chemistry used to form the TA-Ti^{IV} gels and metal–organic frameworks (MOFs) prompted us to investigate if MOF crystallization could be realized in situ during formation of the TA-Ti^{IV} gels. As a proof of concept, MOF-5 and HKUST-1 crystallization[21] within the TA-Ti^{IV} gel system was examined and crystallization—gelation occurred simultaneously without inhibiting each other (Figure 3n–q). As a control, MOF structures in bulk were prepared for comparison (see Figure S8). Differences in the morphologies of the MOF particles (e.g., MOF-5 needles of lengths of ca. 40–60 µm in the gel compared with MOF-5 needles of lengths of 100–150 µm in solution) could be attributed to the spatial influence of the gel matrix on MOF crystallization. The MOF-gel composites are structures which contain both crystalline (MOF) and amorphous (metallogel) coordination networks. Co-formation of such multilevel hybrid structures is rare and provides both new insight into this type of chemistry and the potential for new applications.

In general, the gelation mechanism underlying the formation of metallogels is not completely understood.[22–25] However, we hypothesize that the high oxidation state and formal charge of Ti^{IV} play a significant role in the solvent-trapping process of the gelation,[24–27] in addition to coordinative crosslinking, thus enabling the formation of gel networks. This may explain why Fe^{III} does not form a gel in the presence of TA despite exhibiting the strongest known coordination interactions with catechol-type ligands.[19,28] Additionally, this explanation predicts that other group(IV) metals would form gels upon combination with TA, as indicated by the positive results obtained from preliminary experiments involving Zr^{IV} (see Figure S9). The current results thus provide new insight into the formation of dynamic, coordination-driven metallogels, and represent

a versatile platform for the development of new materials for diverse applications. We are currently exploring these gels for their potential application in drug crystallization and delivery, catalysis, and metal sequestration and environmental remediation.

Acknowledgments

This research was supported by the Australian Research Council (ARC) under the Australian Laureate Fellowship (FL120100030) Scheme, and the ARC Centre of Excellence in Convergent Bio-Nano Science and Technology (Project CE140100036). This work was performed in part at the Materials Characterisation and Fabrication Platform at the University of Melbourne and the Victorian Node of the Australian National Fabrication Facility.

Keywords: chelates · coordination chemistry · gels · organic-inorganic hybrid composites · titanium

How to cite: *Angew. Chem. Int. Ed.* **2016**, *55*, 13803–13807
Angew. Chem. **2016**, *128*, 14007–14011

[1] C. Ortiz, M. C. Boyce, *Science* **2008**, *319*, 1053–1054.
[2] J. Aizenberg, P. Fratzl, *Adv. Mater.* **2009**, *21*, 387–388.
[3] K. Ariga, J. Li, J. Fei, Q. Ji, J. P. Hill, *Adv. Mater.* **2016**, *28*, 1251–1286.
[4] M. J. Harrington, A. Masic, N. Holten-Andersen, J. H. Waite, P. Fratzl, *Science* **2010**, *328*, 216–220.
[5] H. Ejima, J. J. Richardson, K. Liang, J. P. Best, M. P. van Koeverden, G. K. Such, J. Cui, F. Caruso, *Science* **2013**, *341*, 154–157.
[6] J. Guo, Y. Ping, H. Ejima, K. Alt, M. Meissner, J. J. Richardson, Y. Yan, K. Peter, D. von Elverfeldt, C. E. Hagemeyer, F. Caruso, *Angew. Chem. Int. Ed.* **2014**, *53*, 5546–5551; *Angew. Chem.* **2014**, *126*, 5652–5657.
[7] M. A. Rahim, K. Kempe, M. Müllner, H. Ejima, Y. Ju, M. P. van Koeverden, T. Suma, J. A. Braunger, M. G. Leeming, B. F. Abrahams, F. Caruso, *Chem. Mater.* **2015**, *27*, 5825–5832.
[8] M. J. Webber, E. A. Appel, E. W. Meijer, R. Langer, *Nat. Mater.* **2015**, *15*, 13–26.
[9] M.-O. M. Piepenbrock, G. O. Lloyd, N. Clarke, J. W. Steed, *Chem. Rev.* **2010**, *110*, 1960–2004.
[10] X. Du, J. Zhou, J. Shi, B. Xu, *Chem. Rev.* **2015**, *115*, 13165–13307.
[11] N. Holten-Andersen, M. J. Harrington, H. Birkedal, B. P. Lee, P. B. Messersmith, K. Y. C. Lee, J. H. Waite, *Proc. Natl. Acad. Sci. USA* **2011**, *108*, 2651–2655.
[12] N. Holten-Andersen, A. Jaishankar, M. J. Harrington, D. E. Fullenkamp, G. DiMarco, L. He, G. H. McKinley, P. B. Messersmith, K. Y. C. Lee, *J. Mater. Chem. B* **2014**, *2*, 2467–2472.
[13] Q. Li, D. G. Barrett, P. B. Messersmith, N. Holten-Andersen, *ACS Nano* **2016**, *10*, 1317–1324.
[14] H. Ceylan, M. Urel, T. S. Erkal, A. B. Tekinay, A. Dana, M. O. Guler, *Adv. Funct. Mater.* **2013**, *23*, 2081–2090.
[15] S. C. Grindy, R. Learsch, D. Mozhdehi, J. Cheng, D. G. Barrett, Z. Guan, P. B. Messersmith, N. Holten-Andersen, *Nat. Mater.* **2015**, *14*, 1210–1216.
[16] M. Krogsgaard, A. Andersen, H. Birkedal, *Chem. Commun.* **2014**, *50*, 13278–13281.
[17] M. Shin, J. H. Ryu, J. P. Park, K. Kim, J. W. Yang, H. Lee, *Adv. Funct. Mater.* **2015**, *25*, 1270–1278.
[18] P. Tengvall, I. Lundström, *Clin. Mater.* **1992**, *9*, 115–134.
[19] M. J. Sever, J. J. Wilker, *Dalton Trans.* **2004**, 1061–1072.
[20] R. Inde, M. Liu, D. Atarashi, E. Sakai, M. Miyauchi, *J. Mater. Chem. A* **2016**, *4*, 1784–1791.
[21] N. Stock, S. Biswas, *Chem. Rev.* **2012**, *112*, 933–969.
[22] M. Cametti, M. Cetina, Z. Džolić, *Dalton Trans.* **2015**, *44*, 7223–7229.
[23] A. Y.-Y. Tam, V. W.-W. Yam, *Chem. Soc. Rev.* **2013**, *42*, 1540–1567.
[24] L. A. Estroff, A. D. Hamilton, *Chem. Rev.* **2004**, *104*, 1201–1218.
[25] T. D. Hamilton, D.-K. Bučar, J. Baltrusaitis, D. R. Flanagan, Y. Li, S. Ghorai, A. V. Tivanski, L. R. MacGillivray, *J. Am. Chem. Soc.* **2011**, *133*, 3365–3371.
[26] H. Liang, Z. Zhang, Q. Yuan, J. Liu, *Chem. Commun.* **2015**, *51*, 15196–15199.
[27] B. Xing, M.-F. Choi, B. Xu, *Chem. Eur. J.* **2002**, *8*, 5028–5032.
[28] Z. Xu, *Sci. Rep.* **2013**, *3*, 2914.

Received: August 28, 2016
Published online: September 30, 2016

